EXTREME PRECISION LIDAR MAPPING

C. K. Toth[a], D. Grejner-Brzezinska [b], M. Bevis[c]

[a]OSU, Center for Mapping, 1216 Kinnear Road, Columbus, OH 43212-1154, USA – toth@cfm.ohio-state.edu
[b]OSU, Department of Civil and Environmental Engineering and Geodetic Science, Columbus, USA
[c]OSU, Department of Geological Sciences, Columbus, USA

Commission I, WG I/2

KEY WORDS: LiDAR, Airborne Laser Scanning, Georeferencing, QA/QC, Accuracy

ABSTRACT:

To advance earthquake research, a unique LiDAR (Light Detection and Ranging) survey was conducted to map an approximately 1,000 km segment of the San Andreas Fault in southern California in the spring of 2005. The objective was to produce a surface model along the fault line at extremely high accuracy and consequently, extraordinary care was devoted to all the system components and the mission planning of the LiDAR survey. A dense network of GPS reference stations was established in addition to the PBO (Plate Boundary Observation) system to provide short baselines for the sensor platform orientation. The Optech 3100 ALTM system was operated at a 70 kHz pulse rate, which provided an optimum in terms of balancing the requirements for good ranging accuracy, large area coverage and high point density. For quality control, including systematic error corrections, conventional profiles were collected and LiDAR-specific targets were used. These targets not only provided for the vertical correction, but were also able to improve the horizontal accuracy. This paper provides a brief project overview and a preliminary analysis of the achieved accuracy.

1. INTRODUCTION

LiDAR or airborne laserscanning has become the primary surface extraction technique in recent years. Used locally, this technology can deliver dense surface point clouds at excellent vertical accuracy; a vertical accuracy of 10-15 cm can be achieved routinely under typical circumstances. Recent developments in the laser sensor technology have reached the point that rotating mirror-based system can achieve cm-level ranging accuracy. Consequently, the sensor platform orientation errors, or navigation errors of the GPS/IMU georeferencing system have started to account for the major part of the error budget of the LiDAR product. In another interpretation, through eliminating or reducing the navigation errors, it is feasible to approach the ranging accuracy for the LiDAR points on good surfaces – defined as nearly flat areas with specular reflection characteristics. Obviously, mainstream mapping rarely requires such an extraordinary accuracy, yet some subfields could benefit from accuracy. For example, active earthquake areas typically lie along tectonic plate boundaries. In extreme cases, the rate of the motion along the plate boundary lines may reach a few cm per year. Therefore, a surface mapping technology with comparable accuracy performance can have a great potential to observe plate motion and any deformation along the fault lines and could thus advance our understanding to model and predict earthquake processes.

The project B4, codenamed to reference to the "before" status of a widely anticipated major earthquake, the Big One, is a National Science Foundation (NSF) sponsored project, led by scientists from The Ohio State University (OSU) and the U.S. Geological Surveys (USGS), to create an unprecedentedly accurate surface model (DEM) along the San Andreas Fault in southern California. Besides the USGS, the OSU-led team included NCALM (National Center for Airborne Laser Mapping) from the University of Florida, UNAVCO (a non-profit, membership-governed consortium, supporting Earth science) and Optech International.

The team completed an Airborne Laser Swath Mapping (ALSM) survey of ~ 1,000 km of the southern San Andreas Fault and San Jacinto Fault systems in May 2005. The main objectives of this project are (1) to capture in great detail the geometry of the near-field of these faults prior to the Big One, so that after a great earthquake occurs the survey can be repeated to examine the near-field displacements (coseismic and postseismic) in extraordinary detail, and thereby resolve some of the great debates about earthquake source physics, (2) provide our present results to geomorphologists and paleoseismologists, who can use offsets in topography to address the history of major earthquakes along these faults, and to guide the selection of new trenching sites and dating, and (3) improve the near-field geodetic infrastructure of these fault systems. Large numbers of volunteers played a crucial role in the original field measurements, and the indications are that the group of science data users will continue to grow as we move from raw data, through preliminary data products, to the refined and higher level data products.

2. PROJECT AREA

The project is aimed to investigate the primary continental transform fault of the North American – Pacific plate boundary, the southern San Andreas fault (SSAF), see Figure 1, from just northwest of Parkfield to Bombay Beach, California (e.g., Wallace, 1949 and 1990; Matti and Morton, 1993). This section of the fault includes the transition from creeping to locked zones along-strike at the northwestern end, as well as what is known as the Big Bend and both tectonic 'knots' at Tejon Pass and San Gorgonio Pass (e.g., Sykes and Seeber, 1985). Furthermore, it includes perhaps the most heavily primed section of the entire San Andreas Fault that runs down the Coachella Valley to its southeastern terminus at Durmid Hill. Of the many possible "Big Ones" on the southern San Andreas Fault, the acquired dataset is likely to cover them all. If the pre-event imagery obtained by this study were to be differenced with post-event imagery, an unprecedented mapping of the near-fault pattern of

deformation would result in a very high-resolution three-dimensional displacement field along the entire rupture zone.

From Cajon Pass towards the southeast to Whitewater is a section that remains highly controversial, since some investigators believe it has accumulated as much as 14 meters of slip since the last event, whereas others feel that it may have slipped as recently as 1812 or 1857 and hence has little accumulated strain (e.g., McGill and Rubin, 1999). The San Bernardino Mountains to the north, and San Jacinto Mountains to the south, press together across the multiple traces of the San Andreas fault zone. Some 10-15 mm/yr of right-lateral shear strain makes its way around the east end of the Big Bend, from the San Andreas fault in the Coachella Valley (near Indio and Palm Springs) to the Eastern California Shear Zone (ECSZ; near Yucca Valley and Landers). A similar amount may feed from the San Jacinto fault to the Mojave segment of the San Andreas fault (to the northwest of Cajon Pass). The amount of strain occurring within this complex portion is not clear, but may be as little as 5 mm/yr or as much as 15 mm/yr. Recent studies of the Coachella Valley segment confirm that several hundred years have elapsed while the fault continues to accumulate strain at a high rate (e.g., Fumal *et.al.*, 1993), clearly indicative of a strong proclivity towards future seismic rupture.

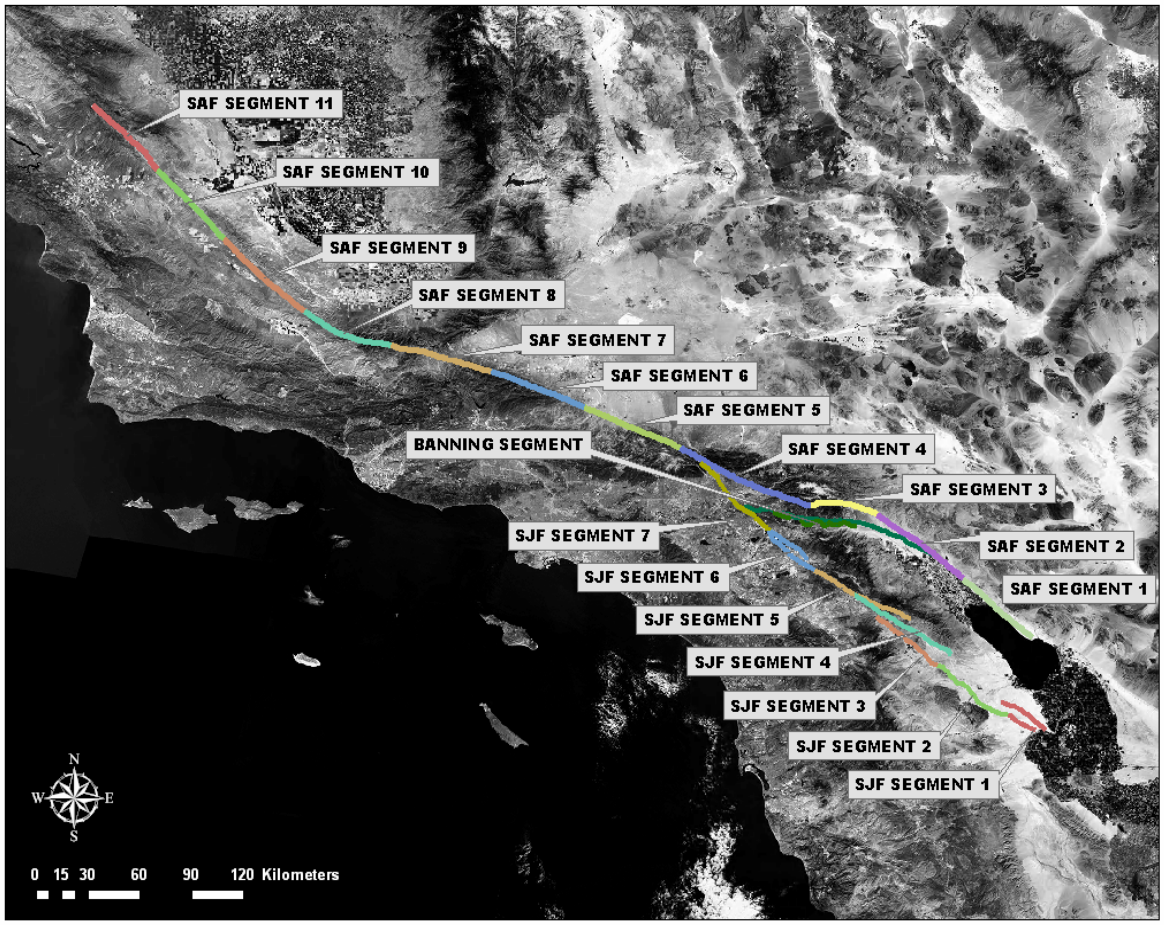

Figure 1. The southern San Andreas and San Jacinto faults; segments show about 50 km sections of the fault lines that were flown over 5-6 times with 50% overlap in a single mission.

3. DATA ACQUISITION CAMPAIGN

The airborne surveys took place May 15-25. 2005. A Cessna 310 aircraft was hired and Optech International provided the ALTM 3100 system at no cost to the project. NCALM was in the charge of the flight operations. OSU was the lead team for the GPS work, which was assisted by UNAVCO and USGS Pasadena staff. The ground LiDAR target and profiling operations were supported by two OSU teams.

The airborne sensor suite included:

- The state-of-the-art Optech 3100 system configured for 70 kHz pulse rate. This represented an optimal balance between the high spatial resolution of the LiDAR points and a good accuracy for the range measurements.
- An experimental color-infrared digital camera was installed next to the Optech 3100 system, providing imagery of 1K by 2K resolution in four bands; images were acquired synchronized to the 1PPS GPS signal (1 FPS).
- In addition to the built-in Applanix POS component of the Optech 3100 system, a Honeywell H764G IMU unit was also installed in the airplane. The increased redundancy offered a potential for improved QA/QC processes, as well as for better combined georeferencing results.

The project area encompassing about 1,000 km of fault line was segmented into smaller sections, including the San Andreas and San Jacinto fault lines (SAF and SJF) as shown in Figure 1. Each segment was about 50 km long and to achieve a swath width of about 1,000 m with double coverage, 5-6 flight lines with 50% overlap were flown. On a typical day, two segments were mapped, each requiring about a net 2 hours of sensor-on time.

To achieve the highest possible georeferencing performance of the airborne platform, a dense network of GPS reference stations was established along the fault line. About 100 new stations were set up at an average spacing of 10 km. The stations were occupied for about 6-10 hours to support the LiDAR flights, as well as to allow for referencing them to the POB system; the POB reference stations close to the fault lines were switched to a 1 Hz data acquisition rate for the duration of the data acquisition campaign.

For QA/QC of the surface points, as well as for the additional LiDAR strip corrections, mobile LiDAR-specific targets were used throughout the surveys. Typically, two clusters of 3-4 targets were placed along the approximately 50 km long flight segments. The target cluster location was planned to be located at around 1/3 and 2/3 of the segment length. However, due to access difficulties, such as excessive drive time or lack of drivable roads, the actual location varied on a wider scale.

The total number of personnel involved in the airborne and ground surveys was about 30, including project leaders from OSU and USGS, staff from NCALM, Optech and UNAVCO, students and volunteers.

4. DATA PROCESSING

The 10 days of intense airborne and ground surveys produced a massive amount of data, presenting a rather complex and time-consuming data processing task for the team. First the GPS reference station network was processed. Subsequently, based on those results, the flight lines were processed, followed by the creation of the initial LiDAR point datasets to meet the delivery of a preliminary product, urgently expected by the earthquake research community. In the second phase, refinements are being applied in every stage of the processing to achieve the highest possible accuracy of the end products. This process is still going on and final results are expected later this year. In the following, a few samples are shown to indicate important aspects and an initial accuracy analysis of the data processing.

4.1 Reference Station Data Processing

The GPS reference station network adjustment was performed at OSU. The GAMIT software was used for this processing task. Initial results were made available in July and the final results were released in October, 2005. The accuracy of the second adjustment resulted in about 3 mm horizontal and 10 mm vertical accuracy, see (Bevis *et.al.*, 2005). Figure 2 shows the GPS reference station locations for the first San Andreas Fault segment; six new stations were installed along the fault line to complement the three POB stations in the area.

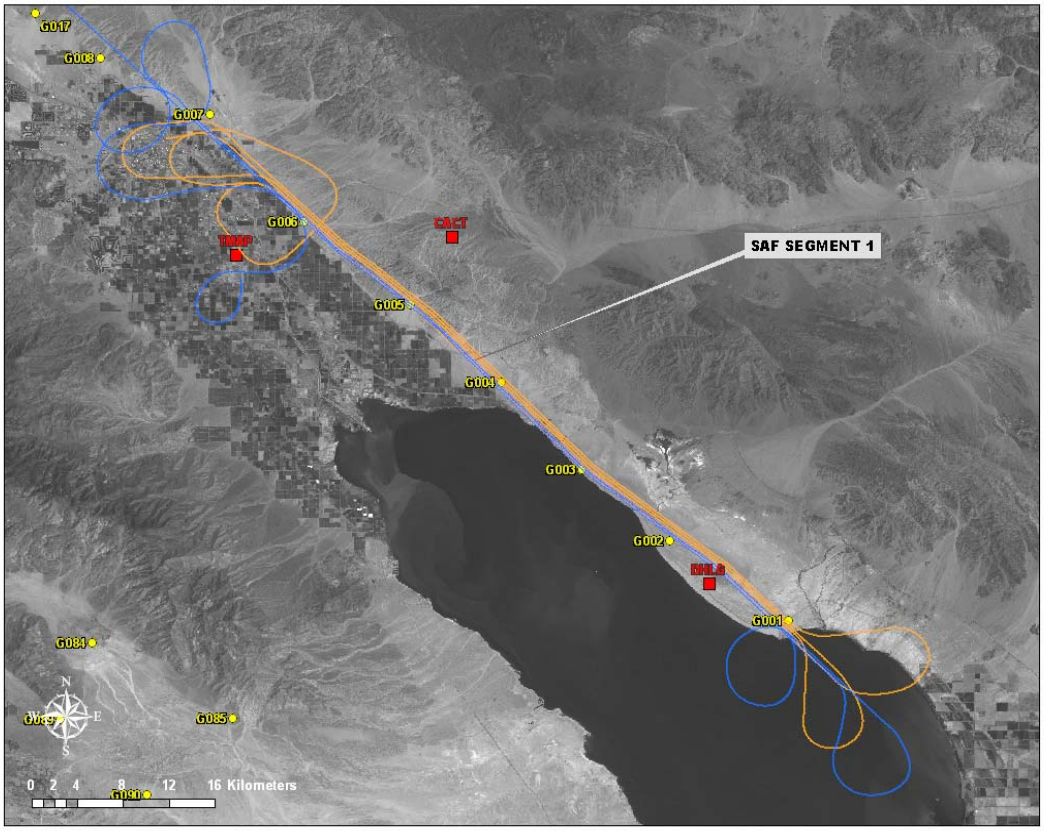

Figure 2. The flight trajectories of the first segment of the San Andreas Fault with GPS reference stations; newly established stations are marked yellow, existing PBO stations are marked red.

4.2 Flight Line Processing

The flight lines were initially processed by the KARS software (Mader, 1992) and the results were used to merge with the Applanix IMU data to provide the sensor orientation for the LiDAR system. To achieve high reliability of the results, two independent groups performed a thorough analysis of select flight line solutions with respect to the base stations used. The objective of the comparative investigation was to decide whether to use double differenced L1 phase solution or L3, ionosphere free solution, and to formulate a method for how to utilize the available base stations along the flight lines for the most accurate solution. The extensive analysis of the baseline length dependence of the L1 and L3 solutions revealed that the RMS value of the L1 phase solution greatly depends on the distance from the base station as expected, while the RMS of the L3 phase solution is practically independent of the baseline length. It was also found that up to about 30 km distance from the base station, generally the RMS of the L1 solution is smaller than the RMS of the L3 solution. Furthermore, the comparison of the solutions computed with different base stations along the flight lines confirmed an about 1-2 cm accuracy of the base station coordinates.

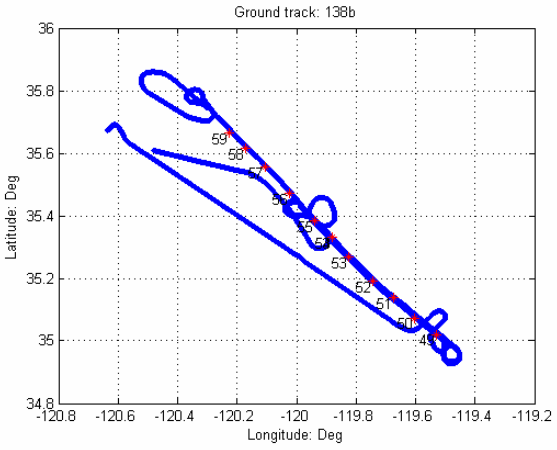

Figure 3. A 100-km flight line with GPS reference stations.

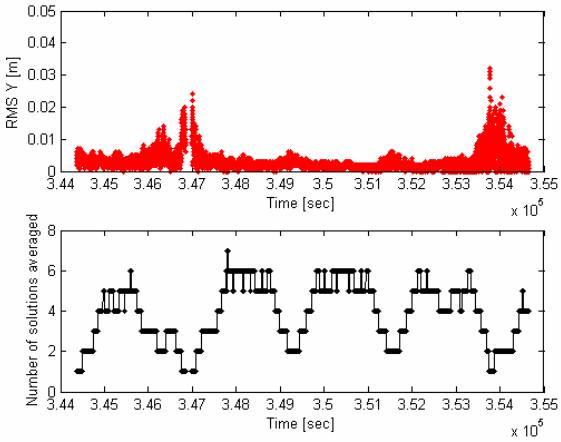

Figure 4. RMS results of the vertical coordinate from the combined solution and the number of base stations used.

To compute the final trajectory from the overlapping solutions with the different base stations, a weighted average was calculated with the weights based on the RMS values of the individual solutions. Due to high redundancy, this method provides a superior solution compared to methods using only one base station and thereby can provide improved accuracy of the final LiDAR product. Figure 3 illustrates an example of a 100 km long flight line (two segments flown together) with the available base stations along the fault approximately 10 km apart, while Figure 4 shows the RMS of the combined solution for the vertical coordinate and the number of base stations used.

4.3 Processing of LiDAR-specific Targets

The sensor georeferencing received unusual attention in the B4 project, as discussed above. But even under this extreme care, ground control is the only way to validate the performance of the LiDAR product. Most of the surveyed SAF and SJF flight lines are in mountainous and desert areas, where there are practically no adequate objects for QA/QC. There are no paved areas or buildings, and the typical coverage is vegetation, ranging from desert shrubs to wooded landscapes. Therefore, LiDAR-specific targets and conventional profiles (transects) were used for ground control, see Figure 5a. A detailed discussion on target design and achievable accuracy can be found in (Csanyi et.al., 2005; Csanyi and Toth, 2006). During the 10-day airborne surveying campaign, LiDAR targets were placed at an average spacing of 15 km along the 1,000 km fault line. The periphery of targets was GPS-surveyed at six positions with a 5-8 minute occupation time for each location. Using the closest GPS reference station, the clusters were computed by KARS; Figure 5b shows the typical results. In subsequent processing steps, outliers were removed and the six locations were computed followed by the derivation of the center location coordinates of the target and the orientation of the target plane. Extended analysis confirmed that the typical accuracy of the target center point is 2-3 cm horizontally and 2 cm vertically.

4.4 Performance Evaluation

The availability of the LiDAR-specific target data allowed for the assessment of the LiDAR point accuracy. Figure 6 shows a cluster of three targets in segment SAF1, using color representation of the elevation data.

A dedicated software utility was developed to automate the extraction of the LiDAR targets from the raw LiDAR point cloud. The program selects without human intervention the target areas from the LiDAR strips, finds the LiDAR points on the targets, and determines the target positions. The extraction of the points falling on the LiDAR targets is accomplished in two steps. First, LiDAR points in the vicinity of the targets are windowed out based on the known (surveyed) target coordinates and the maximum expected errors in the LiDAR data. In the second step, the points not falling on targets are filtered out based on vertical elevation differences and intensity information and subsequently the remaining target candidate points are checked for geometry. The output of the process is the estimated location of the centerpoint of the target. Table 1 below shows the results for the case shown in Figure 6, where target locations automatically extracted from the NCALM provided LiDAR data are compared with the GPS-surveyed target coordinates. The results confirm that a good accuracy was achieved in the overall LiDAR data processing.

a)

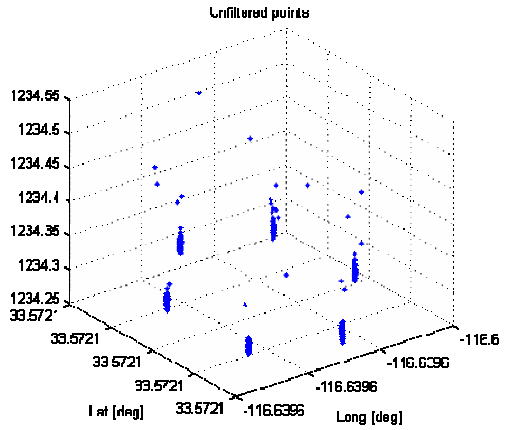

b)

Figure 5: LiDAR-specific target (a) with GPS positioning results (b).

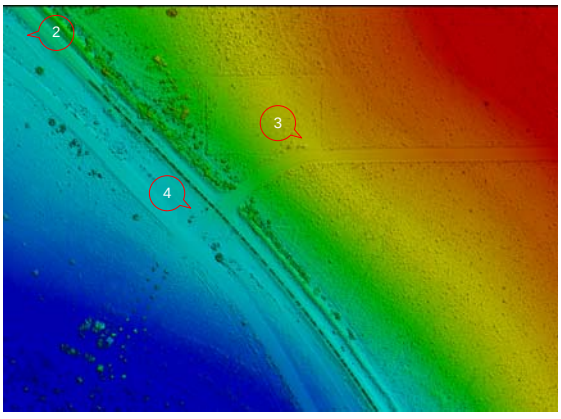

Figure 6: A cluster of three LiDAR targets.

Table 1. Coordinate comparison.

	LiDAR (NCALM) [m]		
	X	Y	Z
2	600381.57	3708592.44	-92.18
3	600712.71	3708469.62	-82.54
4	600579.61	3708382.45	-92.19
	GPS-measured target [m]		
	X	Y	Z
2	600381.55	3708592.56	-92.23
3	600712.44	3708469.71	-82.53
4	600579.70	3708382.60	-92.23
	Differences [m]		
	X	Y	Z
2	0.02	-0.12	0.05
3	0.27	-0.09	-0.01
4	-0.08	-0.15	0.04
Average	**0.07**	**-0.12**	**0.03**
STDEV	**0.18**	**0.03**	**0.03**

5. CONCLUSIONS

The B4 Project Team performed a high-resolution topographic survey of the San Andreas and San Jacinto fault zones in southern California, in order to obtain pre-earthquake imagery necessary to determine near-field ground deformation after a future large event and to support tectonic and paleoseismic research. The B4 project to map the surface along the fault lines at unprecedented accuracy has produced encouraging initial results. The dense GPS reference network combined with meticulous processing resulted in very accurate flight line trajectories and consequently provided an exceptionally small navigation error budget for the LiDAR point processes. Sample data indicate that the vertical LiDAR point accuracy falls in the sub-decimeter range and can be further improved where ground control is available.

ACKNOWLEDGEMENTS:

The B4 project was funded by the National Science Foundation and the ALTM 3100 system was generously provided by Optech international. The authors wish to thank to all the contributing personnel from USGS, NCALM, UNEVCO, and other academic and government institutes and private companies who are not individually listed here for contributing their time and resources to the B4 project.

REFERENCES

Bevis, M. *et.al.*, 2005. The B4 Project: Scanning the San Andreas and San Jacinto Fault Zones, *Eos Trans. AGU, 86*(52), Fall Meet. Suppl., H34B-01,.

Csanyi, N. – Toth, C. – Grejner-Brzezinska, D. – Ray, J., 2005. Improving LiDAR data accuracy using LiDAR-specific ground targets, ASPRS Annual Conference, Baltimore, MD, March 7-11, CD-ROM.

Csanyi, N. – Toth, C., 2006. Improvement of LiDAR Data Accuracy Using LiDAR-Specific Ground Targets, *Photogrammetric Engineering & Remote Sensing*, (in press).

Fumal, T.E. – Pezzopane, S.K. – Weldon, R.J., II, – Schwartz, D.P., 1993. A 100-year average recurrence interval for the San Andreas Fault at Wrightwood, California: *Science*, v. 259, p. 199-203.

Grejner-Brzezinska D. A., 1999. Direct Exterior Orientation of Airborne Imagery with GPS/INS System: Performance Analysis, *Navigation*, Vol. 46, No. 4, pp. 261-270.

Mader, G.L., 1992. Rapid Static and Kinematic Global Positioning System Solutions Using the Ambiguity Function Technique, *Journal of Geophysical Research,* 97, 3271-3283.

Matti, J.C. – Morton, D.M., 1993. Paleogeographic evolution of the San Andreas fault in southern California: a reconstruction based on a new cross-fault correlation, *in* Powell, R.E., Weldon, R.J., and Matti, J.C., eds., The San Andreas fault system: displacement, palinspastic reconstruction, and geologic evolution: *Geological Society of America Memoir 178*, p. 107-159.

McGill, S. F., – C. M. Rubin, 1999. Surficial slip distribution on the central Emerson fault during the June 28, 1992, Landers earthquake, California, *J. Geophys. Res*., vol. 104, #B3, pp. 4811-4833.

Sykes, L.R., – Seeber, L., 1985. Great earthquakes and great asperities, San Andreas fault, southern California: *Geology*, v. 13, no. 12, p. 835-838.

Wallace, R.E., ed., 1990. The San Andreas Fault system, California: *U.S. Geological Survey Professional Paper 1515*, 283 p.

Wallace, R.E., 1949. Structure of a portion of the San Andreas rift in southern California: *Geological Society of America Bulletin*, v. 60, no. 4, p. 781-806.